Am J Transl Res 2025;17(12):9412-9421
www.ajtr.org /ISSN:1943-8141/AJTR0166158

Original Article

A clinical and CT-based model for differentiating high-grade from low-grade lung adenocarcinoma in patients with idiopathic pulmonary fibrosis

Qianli Ma[1], Weina Li[2], Lin Chen[3], Xunhui Zhuang[4]

[1]Department of Oncology, Qingdao Municipal Hospital, Qingdao, Shandong, China; [2]Department of Cardiovascular, Qingdao Eighth People's Hospital, Qingdao, Shandong, China; [3]Department of Oncology Comprehensive Treatment, Qingdao Central Hospital, University of Health and Rehabilitation Sciences (Qingdao Central Hospital), Qingdao, Shandong, China; [4]Department of Radiology, Women and Children's Hospital, Qingdao University, Qingdao, Shandong, China

Received May 19, 2025; Accepted November 24, 2025; Epub December 15, 2025; Published December 30, 2025

Abstract: Objectives: To establish a clinical and CT-based diagnostic model to predict high-grade lung adenocarcinoma (LAC) in patients with idiopathic pulmonary fibrosis (IPF). Methods: A total of 289 LAC-IPF patients were enrolled retrospectively and were divided into training (n=171) and test sets (n=118). In each set, the patients were divided into a low-grade LAC group and high-grade LAC group according to pathologic findings. Clinical and high-resolution CT (HRCT) features were analyzed by binary logistic regression analysis to select independent predictors for high-grade LAC by building three models: the clinical model, the radiologic model, and the combined model integrating the independent clinical and radiologic factors. The discriminative performance of the three models was assessed using the receiver operating characteristic (ROC). The model with the best diagnostic performance was verified in the test set. Results: There was no significant difference between the training and test sets regarding clinical and radiologic factors (P>0.05). The usual interstitial pneumonia (UIP) pattern of IPF, solid morphology of the tumor, cytokeratin 19 fragments (CYFRA21-1, the cutoff value: 2.85 ng/mL) and smoking history were identified as independent predictors for high-grade LAC. The combined model showed the best discriminative performance (AUC: 0.955 in the training set and 0.853 in the test set), with sensitivity, specificity, and accuracy of 94.0%, 87.1%, and 91.2%, respectively. Conclusions: A clinical and CT-based model can be used as an effective tool to predict high-grade LAC in IPF patients.

Keywords: Lung adenocarcinoma, idiopathic pulmonary fibrosis, tomography, X-ray computed

Introduction

Lung adenocarcinoma (LAC), the most prevalent subtype of lung cancer [1], is divided into low-grade and high-grade subtypes according to the 2015 WHO Classification of Lung Tumor [2]. Evidence suggests that in patients of low-grade LAC, segmentectomy or sublobectomy may offer the same long-term survival as lobectomy, without an increase in the risk of local recurrence, whereas lobectomy or unilateral lung resection is recommended for high-grade LAC patients [3].

Idiopathic pulmonary fibrosis (IPF) is considered an independent risk factor for the development of lung cancer [4]. Epidemiologic evidence suggests that patients with IPF exhibit a fivefold higher risk for developing lung cancer compared to the general population [5], and their mortality (8.00%-17.31%) exceeds that of lung cancer patients without IPF [4]. Furthermore, the reported prevalence of lung cancer in patients with IPF seems to increase over the clinical course of IPF, with the cumulative incidence exceeding 50% at 10 years of follow-up [6]. Thus, preoperative diagnosis of high-grade LAC in patients with IPF (LAC-IPF) is of great importance. However, LAC and IPF share overlapping symptoms, and the imaging features of LAC are atypical when superimposed on the

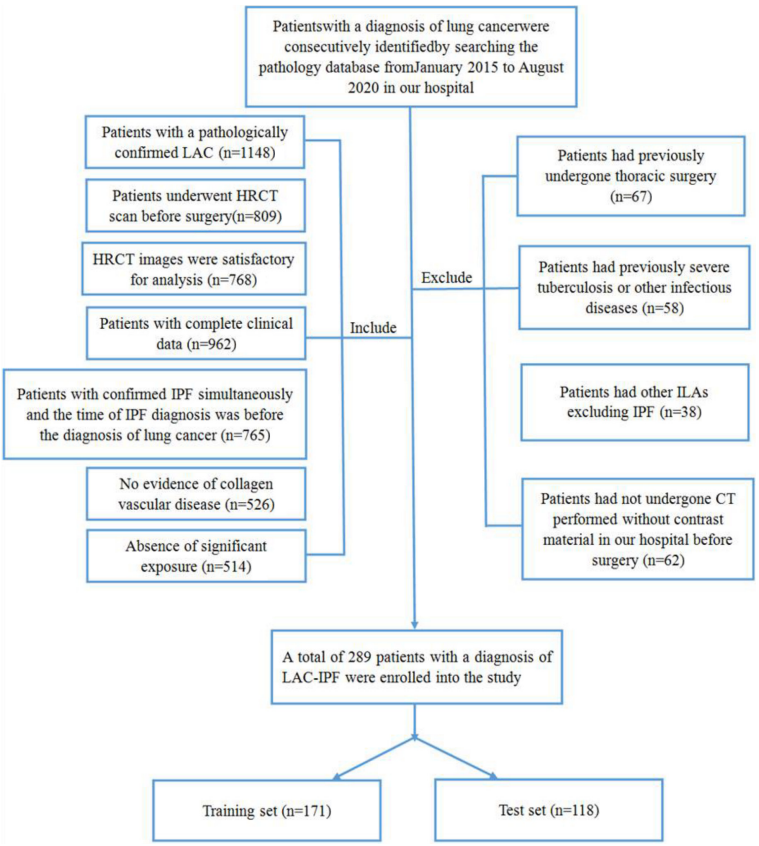

Figure 1. Flow chart for study population selection. Notes: LAC, high-grade lung adenocarcinoma; HRCT, high-resolution computed tomography.

fibrotic background of IPF, making early diagnosis of LAC-IPF challenging.

The pathology, mechanism, and the prognosis of LAC-IPF have been reported by large cohort studies [1, 7]. However, few studies have focused on the radiologic features of LAC-IPF on high-resolution computed tomography (HRCT), especially the differences between low-grade LAC and high-grade LAC. Iwasawa et al. [8] demonstrated that the quantitative assessment of fibrosis extent in interstitial lung abnormalities (ILAs) on preoperative CT is useful for evaluating the severity of ILAs and for risk stratification in patients with lung cancer. Unfortunately, the differences between low-grade LAC and high-grade LAC on HRCT remains lacking.

This study aimed to investigate whether a model integrating clinical factors and CT characteristics could accurately predict high-grade LAC in patients with IPF on preoperative HRCT.

Materials and methods

Study population

This retrospective study was approved by the ethics committee of Qingdao Municipal Hospital (2024-KY104-108), and the informed patient consent was waived. Consecutive patients who underwent lung cancer surgery from January 2015 to August 2020 in Qingdao Municipal Hospital were potential candidates. Inclusion criteria: (1) pathologically confirmed LAC; (2) preoperative HRCT before surgery; (3) qualified HRCT images for analysis; (4) complete clinical data available; (5) concomitant diagnosis of IPF, with IPF confirmed prior to the diagnosis of lung cancer according to *Fleischner Society White Paper* [9]; (6) no evidence of collagen vascular disease; (7) absence of significant occupational or medication-related exposures. Exclusion criteria: (1) a history of thoracic surgery; (2) a history severe tuberculosis or other infectious diseases; (3) presence of interstitial lung abnormalities other than IPF; (4) absence of preoperative non-contrast HRCT scan performed at our institution.

The final study population comprised 289 patients who underwent video-assisted thoracic surgery for LAC-IPF (160 males and 129 females; median age of 62.1 years (27-83)). According to the time of surgery in LAC-IPF patients, 171 patients from January 2015 to December 2017 comprised the training set, whereas 118 patients from January 2018 to August 2020 constituted the test set. A flow chart for selecting the study population is shown in **Figure 1**. In the training and test sets, the patients were divided into two groups (low-grade LAC-IPF group and high-grade LAC-IPF group). The LAC with the lepidic, acinar, papillary, minimally invasive and preinvasive growth patterns are defined as low-grade subtypes, whereas the tumors displaying micropapillary,

solid, invasive mucinous, colloid, fetal and enteric growth patterns were regarded as high-grade subtypes.

Clinical information included age, sex, smoking status, symptoms (cough, bloody phlegm), which were obtained by searching medical records. Laboratory findings included carcinoembryonic antigen (CEA), cytokeratin 19 fragments (CYFRA21-1), and carbohydrate antigen 125 (CA125).

HRCT image acquisition

All preoperative scans were obtained using a 64-row multidetector scanner (GE Healthcare, Milwaukee, WI, USA) with the following parameters: 120 kVp, 120 mA-200 mA, 1.5-mm collimation, 0.984:1 pitch, reconstruction matrix of 512×512, slice thickness of 1.0 mm, high spatial resolution algorithm, and window width/level 1500/-600 HU for the lung window, 400/40 HU for the mediastinal window.

HRCT characteristics

The HRCT images were independently evaluated by two radiologists (reader 1, J.L., 30 years of experience; and reader 2, X.L., 8 years of experience in CT interpretation). Blinded to the clinical and pathologic information, the two readers interpreted the following CT characteristics by consensus using a picture archiving and communication system (PACS): tumor size (the maximum diameter of the tumor were measured on the axial CT image), IPF pattern (typical usual interstitial pneumonia (T-UIP) pattern characterized by reticular opacities with obligatory honeycombing, usually associated with traction bronchiectasis, and with a basal and subpleural and lower zone predominance; or probable usual interstitial pneumonia (P-UIP) pattern defined as the presence of reticular abnormality and traction bronchiectasis with a basal, subpleural and lower zone predominance, and without honeycombing, according to *Diagnostic Criteria for Idiopathic Pulmonary Fibrosis: A Fleischner Society White Paper* [9], lobe location (lower lobe, upper/middle lobe), distribution ("peripheral location" was defined as the tumor located in the outer one-third of lung, while "central location" was diagnosed when the lesion extended to the inner two-thirds of the lung), lobulation (present or absent, defined as irregular undulation of the nodule margin), spiculation (present or absent, defined as the presence of 2 mm or thicker strands extending from the margin of nodule into the lung parenchyma without touching the pleural surface), bubble lucency (present or absent, defined as small spots of ovoid or round air attenuation in a nodule), air bronchogram (present or absent, defined as an air-filled bronchi within a nodule), pleural indentation (present or absent, defined to a triangular or linear strand starting from the nodule surface and arriving at the pleural surface), vessel convergence (present or absent, defined as multiple blood vessels focused on a nodule), lymph node enlargement (present or absent, defined as showing a size of more than 10 mm on the short axis based on the American Thoracic Society definitions [10]), and CT morphology of the nodule (solid nodule or ground-glass nodule [GGN]; with GGNs classified as pure GGNs (pGGNs) and mixed GGNs (mGGN) [11]).

Building of the clinical factors model

The differences in clinical factors between low-grade and high-grade LAC-IPF groups were assessed using univariate analysis, and variables showing statistical significance were entered into a binary logistic regression model to construct the clinical factors model. Odds ratios (ORs) were calculated for each independent factor, and the relative risk with 95% confidence intervals (CIs) was estimated.

Construction of the radiologic model

Similarly, the radiologic features with significant differences between the two groups, screened out by a univariate analysis, were entered into a binary logistic regression model to select the most valuable features. The selected features were applied to build a radiologic model.

Development of a combined model of clinical factors and radiologic features and assessment of the performance of different models

A combined model integrating significant clinical variables and radiologic features was constructed using binary logistic regression analysis, following the same analytical procedures described above. For each of the three models (clinical model, radiologic model, and the com-

Table 1. Comparison of clinical factors and radiologic factors between low- and high-grade LAC patients in the training set

Item		Total	Low-grade LAC group (n=70)	High-grade LAC group (n=101)	*P* Value
Sex	Male	93	32 (45.7%)	61 (60.4%)	0.058
	Female	78	38 (54.2%)	40 (39.6%)	
Age (y)			45.3±15.9	54.0±16.1	0.226
Smoking	Present	84	10 (14.3%)	74 (73.3%)	0.001
	Absent	87	60 (85.7%)	27 (26.7%)	
Bloody phlegm	Present	32	5 (7.1%)	27 (26.7%)	0.001
	Absent	138	65 (92.9%)	73 (72.3%)	
CEA	Increased	95	34 (48.6%)	61 (60.4%)	0.126
	Absent	76	36 (51.4%)	40 (39.6%)	
CYFRA21-1	Increased	89	9 (12.9%)	80 (79.2%)	0.001
	Absent	82	61 (87.1%)	21 (20.8%)	
CA125	Increased	91	17 (24.3%)	74 (73.3%)	0.001
	Absent	80	53 (75.7%)	27 (26.7%)	
Tumor size			17.82±1.03	33.64±1.14	0.000
IPF-pattern	UIP	24	4 (5.7%)	20 (19.8%)	0.009
	P-UIP	147	66 (94.3%)	81 (80.2%)	
Location	Lower lobe	72	25 (35.7%)	47 (46.5%)	0.159
	Upper/Middle lobe	99	45 (64.3%)	54 (53.4%)	
Morphology	Solid nodule	112	18 (25.7%)	94 (93.1%)	0.001
	pGGN/mGGN	59	52 (74.3%)	7 (6.9%)	
Distribution	Peripheral	121	52 (74.3%)	69 (68.3%)	0.399
	Central	50	18 (25.7%)	32 (31.7%)	
Lobulation	Present	112	40 (57.1%)	72 (71.3%)	0.056
	Absent	59	30 (42.9%)	29 (28.7%)	
Spiculation	Present	62	21 (30.0%)	41 (40.6%)	0.156
	Absent	109	49 (70.0%)	60 (59.4%)	
Bubble lucency	Present	58	26 (37.1%)	32 (31.7%)	0.458
	Absent	113	44 (62.9%)	69 (68.3%)	
Air bronchogram	Present	71	33 (47.1%)	38 (37.6%)	0.214
	Absent	100	37 (52.9%)	63 (62.4%)	
Pleural indentation	Present	89	31 (44.3%)	58 (57.4%)	0.091
	Absent	82	39 (55.7%)	43 (42.6%)	
Vessel convergence	Present	129	49 (70.0%)	80 (79.2%)	0.169
	Absent	42	21 (30.0%)	21 (20.8%)	
Lymph node enlargement	Present	54	0 (0.00%)	54 (53.5%)	0.001
	Absent	117	70 (100.0%)	47 (46.5%)	

Notes: CEA, carcinoembryonic antigen; CA125, carbohydrate antigen 125; CYFRA21-1, cytokeratin 19 fragments; IPF, idiopathic pulmonary fibrosis; UIP, usual interstitial pneumonia; P-UIP, possible usual interstitial pneumonia pattern; pGGN, pure ground-glass nodule; mGGN, mixed ground-glass nodule.

bined model), the diagnostic performance in distinguishing low-grade from high-grade LAC-IPF was evaluated in the training set using receiver operator characteristic (ROC) curve analysis. The cutoff value, area under the curve (AUC), sensitivity, specificity, and overall accuracy for identifying high-grade LAC-IPF were calculated.

Univariate analysis was subsequently performed to compare differences in clinical and CT features between the training and test sets

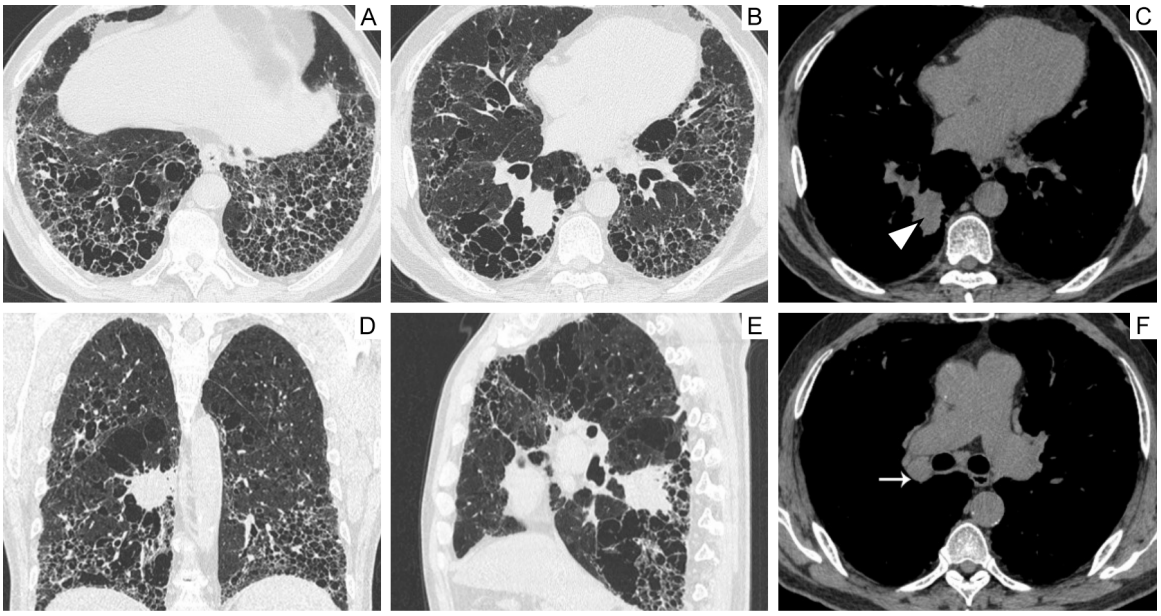

Figure 2. A 59-year male patient with LAC in the test set, showing T-UIP pattern of IPF. (A-C) Axial chest CT showed a solitary solid nodule (white arrow head) located in the lower lobe of the right lung. Coronal (D) and sagittal (E) HRCT show lobulation, spiculation and vessel convergence. Lymph node enlargements are shown in the right hilus of lung with white arrow (F). Notes: LAC, high-grade lung adenocarcinoma; T-UIP, typical usual interstitial pneumonia; IPF, idiopathic pulmonary fibrosis; HRCT, high-resolution computed tomography.

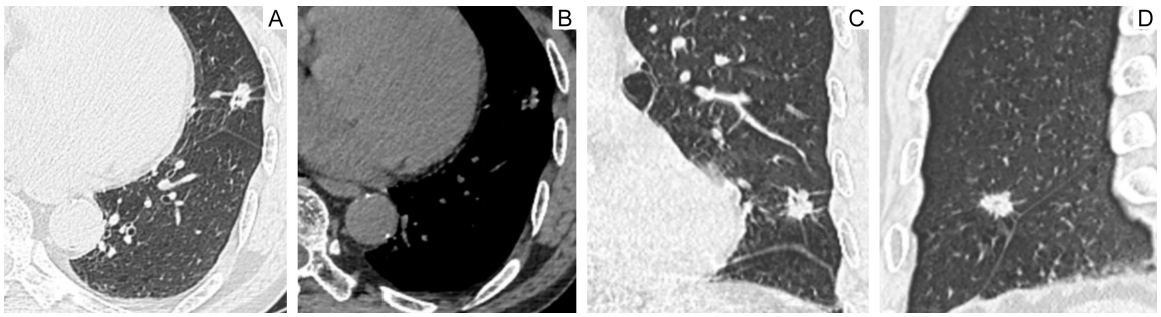

Figure 3. A 66-year male patient of low-grade LAC with IPF from the test set. (A, B) Axial chest CT images show a soft tissue nodule located in the upper lobe of the left lung. (C) Coronal and (D) sagittal CT show the tumor with lobulation, speculation, bubble lucency, and pleural indentation. Notes: LAC, high-grade lung adenocarcinoma; IPF, idiopathic pulmonary fibrosis.

in both low-grade and high-grade LAC-IPF groups. The model with the best diagnostic performance was verified in the test set, and the AUC was obtained.

Statistical analysis

All statistical analyses were performed using SPSS 20.0 (IBM Corp., Armonk, NY, USA). Categorical variables were described as frequency and percentages, and quantitative variables were described using the mean (SD) or median (interquartile range, IQR). The chi-square test or Fisher's exact test were used for comparison between categorical variables. For the logistic regression analysis, quantitative variables were converted into categorical variables according to the cutoff value. Binary logistic regression was then performed to identify clinical and CT features associated with high-grade LAC-IPF. Variables that remained significant were incorporated into model construction. ROC analysis was used to determine its sensitivity, specificity, and accuracy for identifying high-grade LAC-IPF. DeLong test was performed to compare AUCs among the three

Table 2. Binary logistic analysis of the combined model for high-grade LAC in the training set

Item	Odds Ratio	*P* Value
Tumor size	4.405	0.054
IPF-pattern	5.188	0.020
Morphology	21.405	0.002
Lymph node enlargement	53.906	0.997
Smoking	9.842	0.005
Bloody phlegm	0.744	0.766
CYFRA21-1	0.047	0.007
CA125	1.488	0.585
Constant	0.011	0.001

Notes: CA125, carbohydrate antigen 125; CYFRA21-1, cytokeratin 19 fragments; IPF, idiopathic pulmonary fibrosis.

models. A *P* value <0.05 was considered significant.

Results

Building of the clinical model

The clinical factors of patients in the low-grade and high-grade LAC-IPF groups of the training set are provided in **Table 1**. Binary logistic regression analysis identified smoking, CYFRA21-1, and CA125 as independent predictors in the clinical model (*P*=0.001, 0.001 and 0.004, respectively). LAC-IPF patients with smoking history (OR=8.125; 95% CI: 3.305-21.751), increased CYFRA21-1 (OR=7.480; 95% CI: 2.770-20.195; cutoff=2.85 ng/mL from ROC curve analysis), and increased CA125 (OR=4.212; 95% CI: 1.577-11.250; cutoff =13.91 U/mL from ROC curve analysis) were more likely to develop a high-grade of LAC.

Construction of the radiologic model

Of the 12 radiologic features included in this study, four imaging factors (tumor size (with a cutoff of 25 mm in this study), IPF pattern, morphology, and lymph node enlargement) were entered into the binary logistic regression model to select the most valuable features (**Table 1**). The radiologic model was built using three radiological features: tumor size (OR=4.599; 95% CI: 1.286-16.450; *P*=0.019), the T-UIP pattern of IPF (OR=5.118; 95% CI: 1.584-16.539; *P*=0.006), and solid morphology (OR=18.118; 95% CI: 3.462-94.817; *P*=0.001), which were likely to indicate the high-grade LAC-IPF. The imaging characteristics of high-grade and low-grade LAC-IPF are shown in **Figures 2**, **3**.

Construction of a combined model integrating clinical and radiologic features

Four independent predictors, including T-UIP pattern of IPF, solid morphology of the tumor, smoking history, and increased CYFRA21-1, for high-grade LAC in LAC-IPF patients (*P*<0.001) were used to establish a combined model (**Table 2**).

The diagnostic performance of the clinical model, radiologic model, and combined model is summarized in **Table 3**. The AUC of the combined model (0.955; **Figure 4**) was higher than that of the clinical model (0.890; z=3.342, *P*=0.001) and the radiologic model (0.939; z=2.373, *P*=0.018) in the training set. The sensitivity (94.0%), specificity (87.1%) and accuracy (91.2%) of the combined model also outperformed the other two models (**Table 3**).

Validation of the combined model in the test set

There was no significant difference between the training and test sets regarding the clinical and radiologic factors in both the low-grade and high-grade LAC-IPF groups (*P*>0.05, **Table 4**). The combined model also yielded a robust diagnostic performance in the test set, with an AUC of 0.853 (**Figure 5**).

Discussion

The high incidence and poor survival of lung cancer in patients with IPF [6, 12] emphasize the importance of establishing a surveillance protocol for early diagnosis. Given that overlapping pathogenic mechanisms and molecular pathways between lung cancer and IPF [13], diagnosing lung cancer in IPF patients is particularly challenging. The present study shows that the combined model, which incorporates the radiologic signature and clinical factors, has favorable predictive value for the diagnosis of high-grade LAC in IPF patients, with AUCs of 0.890, 0.939 and 0.955 for the clinical model, radiologic model, and combined model, respectively.

One of the most noteworthy findings in our study was that the T-UIP pattern of IPF had a

Table 3. Diagnostic performance of the clinical model, radiologic model, and combined model for high-grade LAC in the training set

Model	Cutoff	AUC (95% CI)	Sensitivity	Specificity	Accuracy
Clinical model	0.381	0.890 (0.835, 0.946)	88.0%	85.7%	87.1%
Radiologic model	0.567	0.911 (0.864, 0.958)	91.1%	84.3%	88.3%
Combined model	0.522	0.955 (0.926, 0.984)	94.0%	87.1%	91.2%

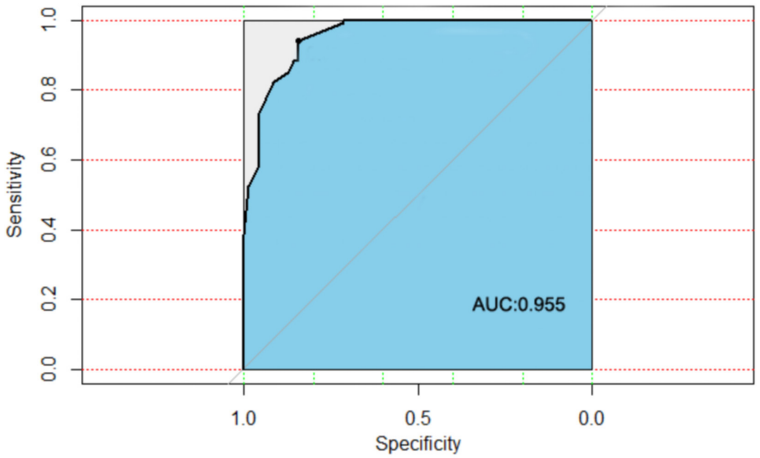

Figure 4. Receiver operator characteristic (ROC) curve of the combined model integrating clinical and radiologic features in the training set.

tendency toward high-grade LAC. To our best knowledge, this was the first study to evaluate and demonstrate the relationship between IPF pattern and the differentiation degree of LAC. Although the mechanism underlying this association remains unclear, several studies have confirmed that IPF and lung cancer share similar pathogenesis of tissue damage and abnormal repair, which are key factors in the development of LAC. This may explain the susceptibility of IPF patients to lung cancer [7, 13, 14]. In addition, aberrant proliferation and tissue invasion of sub-epithelial lung fibroblasts in IPF have close association with cancer biology [7, 14]. Recent advances in molecular techniques also offer genetic and epigenetic-level evidence that abnormal DNA methylation and histone modification leading to abnormal gene expression or aberrant activation of signaling pathways are common to both IPF and lung cancer [15]. Thus, patients with a T-UIP pattern of IPF may be more prone to high-grade LAC. However, further studies are warranted to confirm this hypothesis.

Solid tumor morphology on HRCT, as an independent predictor for high-grade LAC, achieved the highest OR of 21.405 among the significant predictors in the combined model of clinical and radiologic factors, highlighting the substantial contribution of solid morphology to the prediction of high-grade LAC in IPF patients. A study showed that, based on the proportion of the solid component, it may be possible to differentiate between invasive and noninvasive LAC [16]. Yoshida et al. reported that the micropapillary subtype of LAC, regarded as high-grade LAC according to the 2015 WHO classification [17], were observed in 76.2% (16/21) cases with solid nodules [18], consistent with our study (93.1%). In malignant pGGN and mGGN, the solid areas of mGGN histologically represents minimal invasion, while the pure ground-glass nodule areas are considered as lepidic components of adenocarcinoma, which are associated with low-grade LAC subtypes [3]. Therefore, the uneven distribution of different histological subtypes, as Tsubokawa et al. reported [19], may account for the observed variations in HRCT morphology. LAC in the low-grade group tends to grow along the alveolar wall. Due to the slow growth speed of tumor cells, the alveolar spaces are usually incompletely filled with tumor cells and a small amount of gas, resulting in the tumor showing ground-glass nodule on HRCT. Conversely, the tumor cells of high-grade LAC grow rapidly and the alveolar cavity is completely filled with tumor cells. Owing to no gas remaining in the alveolar cavities, the tumor manifests as a solid nodule on HRCT in most cases [3].

In the current study, fragment of cytokeratin 19 (CYFRA 21-1), with a cutoff value of 2.85 ng/mL, was found to be an independent predictor for high-grade LAC. CYFRA 21-1 is essential for structural integrity of epithelial cells, which are expressed in simple epithelium, including the

Table 4. Comparison of clinical and radiologic factors between the patients in the training and test sets stratified by low- and high-grade LAC patients

Item	Low-grade LAC group (n=118)		High-grade LAC group (n=171)	
	χ^2	*P* Value	χ^2	*P* Value
Sex	0.394	0.530	0.106	0.745
Age (y)	0.196	0.658	0.285	0.593
Smoking	1.016	0.314	1.787	0.181
Bloody phlegm		0.670	1.505	0.220
CEA	0.012	0.911	0.133	0.716
CYFRA21-1	0.146	0.702	0.292	0.589
CA125	0.128	0.721	3.336	0.068
Tumor size	0.655	0.418	0.600	0.438
IPF-pattern		0.672	1.162	0.281
Location	0.279	0.598	2.168	0.141
Morphology	1.210	0.271	0.000	1.000
Distribution	1.064	0.302	0.040	0.841
Lobulation	2.445	0.118	0.697	0.404
Spiculation	1.581	0.209	0.336	0.562
Bubble lucency	0.057	0.811	2.419	0.120
Air bronchogram	2.730	0.098	0.762	0.383
Pleural indentation	0.818	0.366	1.527	0.216
Vessel convergence	0.039	0.843	1.179	0.278
Lymph node enlargement		0.514	0.396	0.529

Notes: CEA, carcinoembryonic antigen; CA125, carbohydrate antigen 125; CYFRA21-1, cytokeratin 19 fragments; IPF, idiopathic pulmonary fibrosis.

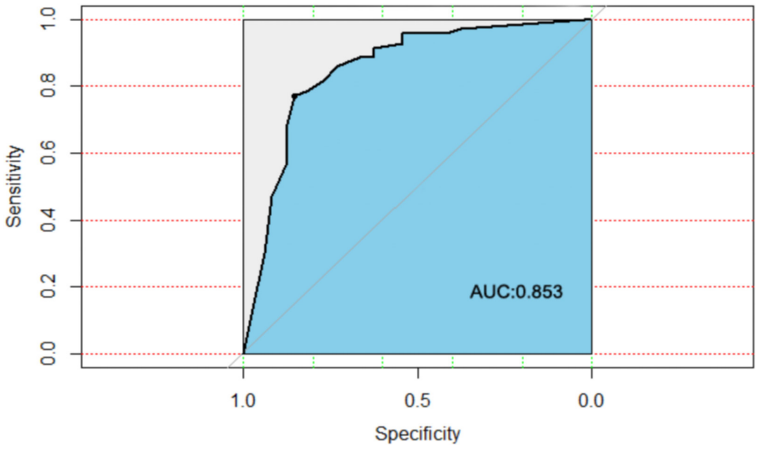

Figure 5. ROC curve of the combined model in the test set.

bronchial epithelium, and in malignant tumors derived from these cells. As a serum cytokeratin 19 fragment, CYFRA 21-1 has been well documented as one of the most single related tumor markers of LAC [20, 21]. In addition, it has been proven that the serum CYFRA 21-1 level varied significantly according to the histologic subgroup of non-small cell lung cancer [22]. A meta-analysis suggests that CYFRA 21-1 has a relatively high diagnostic value (specificity=94%, AUC=0.971) for LAC [23], which is higher than other tumor markers, such as CA-125. Furthermore, CYFRA 21-1 is recognized as a prognostic and predictive marker in LAC [24, 25]. To our knowledge, CYFRA 21-1 has rarely been reported as an independent predictor for the differentiation of LAC. Further studies are warranted to confirm this view. Compared to established LAC grading models, such as the IASLC grading system [26] and radiomic signatures by Song et al. [27], our model demonstrates comparable specificity (87.1% vs 82-90%). However, it requires further validation against pathologic subtyping benchmarks. Notably, unlike existing models designed for general populations, ours specifically addresses the unique challenge of IPF-LAC differentiation where conventional CT features may be obscured by fibrotic changes.

There are several limitations to this study. First, this was based on a modest-sized case series of patients derived from a single hospital, and multi-center studies with larger sample sizes are required for further validation. Second, as a retrospective case-control study, diagnostic accuracy is usually overestimated in the training set. Third, some clinical factors were not included due to incomplete data, such as the duration and severity of smoking, and the IPF severity (e.g., pulmonary function indices). The absence of molecular markers (e.g. EGFR/ALK) and pulmonary function indices in our model represents a limitation, as these factors are established predictors of LAC aggressiveness [28-30]. Fourth, this study did not assess prog-

nostic outcomes (e.g. disease-free survival, overall survival), precluding validation of the association between high-grade LAC and adverse prognosis, thus diminishing the clinical relevance of our model. Future prospective studies should prioritize comprehensive data collection to address these gaps.

Conclusion

In this study, we developed a combined model integrating clinical and radiologic features that showed favorable predictive efficacy in preoperative differentiation of low-grade LAC from high-grade LAC. Patients with a smoking history, high level of CYFRA 21-1, solid tumor morphology and T-UIP pattern of IPF, especially the T-UIP pattern, may be strongly predictive of high-grade LAC. This finding requires further validation before its widespread application in clinical practice.

Disclosure of conflict of interest

None.

Abbreviations

IPF, Idiopathic pulmonary fibrosis; LAC, Lung adenocarcinoma; LAC-IPF, Lung adenocarcinoma in patients with idiopathic pulmonary fibrosis; HRCT, High-resolution computed tomography; ILAs, Interstitial lung abnormalities; CEA, Carcinoembryonic antigen; CYFRA21-1, Cytokeratin 19 fragments; CA125, Carbohydrate antigen 125; PACS, Picture archiving and communication system; T-UIP, Typical usual interstitial pneumonia; P-UIP, Possible usual interstitial pneumonia pattern; GGN, Ground-glass nodule; pGGN, Pure ground-glass nodule; mGGN, Mixed ground-glass nodule; OR, Odds ratio; CI, Confidence interval; ROC, Receiver operator characteristic; AUC, Area under the curve; EGFR, Epidermal growth factor receptor; ALK, Anaplastic lymphoma kinase.

Address correspondence to: Xunhui Zhuang, Department of Radiology, Women and Children's Hospital, Qingdao University, No. 217, Liaoyang West Road, Qingdao 266003, Shandong, China. E-mail: zhuangxh321@163.com

References

[1] Mimae T, Suzuki K, Tsuboi M, Ikeda N, Takamochi K, Aokage K, Shimada Y, Miyata Y and Okada M. Severity of lung fibrosis affects early surgical outcomes of lung cancer among patients with combined pulmonary fibrosis and emphysema. Medicine (Baltimore) 2016; 95: e4314.

[2] Travis WD, Brambilla E, Nicholson AG, Yatabe Y, Austin JHM, Beasley MB, Chirieac LR, Dacic S, Duhig E, Flieder DB, Geisinger K, Hirsch FR, Ishikawa Y, Kerr KM, Noguchi M, Pelosi G, Powell CA, Tsao MS and Wistuba I; WHO Panel. The 2015 World Health Organization Classification of lung tumors: impact of genetic, clinical and radiologic advances since the 2004 classification. J Thorac Oncol 2015; 10: 1243-1260.

[3] Chen D, Dai C, Kadeer X, Mao R, Chen Y and Chen C. New horizons in surgical treatment of ground-glass nodules of the lung: experience and controversies. Ther Clin Risk Manag 2018; 14: 203-211.

[4] Brown SW, Dobelle M, Padilla M, Agovino M, Wisnivesky JP, Hashim D and Boffetta P. Idiopathic pulmonary fibrosis and lung cancer. A systematic review and meta-analysis. Ann Am Thorac 2019; 16: 1041-1051.

[5] Tzouvelekis A, Karampitsakos T, Gomatou G, Bouros E, Tzilas V, Manali E, Tomos I, Trachalaki A, Kolilekas L, Korbila I, Tomos P, Chrysikos S, Gaga M, Daniil Z, Bardaka F, Papanikolaou IC, Euthymiou C, Papakosta D, Steiropoulos P, Ntolios P, Tringidou R, Papiris S, Antoniou K and Bouros D. Lung cancer in patients with idiopathic pulmonary fibrosis. A retrospective multicenter study in Greece. Pulm Pharmacol Ther 2020; 60: 101880.

[6] Ozawa Y, Suda T, Naito T, Enomoto N, Hashimoto D, Fujisawa T, Nakamura Y, Inui N, Nakamura H and Chida K. Cumulative incidence of and predictive factors for lung cancer in IPF. Respirology 2009; 14: 723-728.

[7] Tzouvelekis A, Gomatou G, Bouros E, Trigidou R, Tzilas V and Bouros D. Common pathogenic mechanisms between idiopathic pulmonary fibrosis and lung cancer. Chest 2019; 156: 383-391.

[8] Iwasawa T, Okudela K, Takemura T, Fukuda T, Matsushita S, Baba T, Ogura T, Tajiri M and Yoshizawa A. Computer-aided quantification of pulmonary fibrosis in patients with lung cancer: relationship to disease-free survival. Radiology 2019; 292: 489-498.

[9] Lynch DA, Sverzellati N, Travis WD, Brown KK, Colby TV, Galvin JR, Goldin JG, Hansell DM, Inoue Y, Johkoh T, Nicholson AG, Knight SL, Raoof S, Richeldi L, Ryerson CJ, Ryu JH and Wells AU. Diagnostic criteria for idiopathic pulmonary fibrosis: a fleischner society white paper. Lancet Respir Med 2018; 6: 138-153.

[10] Glazer GM, Gross BH, Quint LE, Francis IR, Bookstein FL and Orringer MB. Normal mediastinal lymph nodes: number and size according to American Thoracic Society mapping. AJR Am J Roentgenol 1985; 144: 261-265.

[11] Hansell DM, Bankier AA, MacMahon H, McLoud TC, Müller NL and Remy J. Fleischner society: glossary of terms for thoracic imaging. Radiology 2008; 246: 697-722.
[12] Yoo H, Jeong BH, Chung MJ, Lee KS, Kwon OJ and Chung MP. Risk factors and clinical characteristics of lung cancer in idiopathic pulmonary fibrosis: a retrospective cohort study. BMC Pulm Med 2019; 19: 149.
[13] Kinoshita T and Goto T. Molecular mechanisms of pulmonary fibrogenesis and its progression to lung cancer: a review. Int J Mol Sci 2019; 20: 1461.
[14] Vancheri C, Failla M, Crimi N and Raghu G. Idiopathic pulmonary fibrosis: a disease with similarities and links to cancer biology. Eur Respir J 2010; 35: 496-504.
[15] Antoniou KM, Tomassetti S, Tsitoura E and Vancheri C. Idiopathic pulmonary fibrosis and lung cancer: a clinical and pathogenesis update. Curr Opin Pulm Med 2015; 21: 626-633.
[16] Asamura H, Hishida T, Suzuki K, Koike T, Nakamura K, Kusumoto M, Nagai K, Tada H, Mitsudomi T, Tsuboi M, Shibata T and Fukuda H; Japan Clinical Oncology Group Lung Cancer Surgical Study Group. Radiographically determined noninvasive adenocarcinoma of the lung: survival outcomes of Japan Clinical Oncology Group 0201. J Thorac Cardiovasc Surg 2013; 146: 24-30.
[17] Mansuet-Lupo A, Bobbio A, Blons H, Becht E, Ouakrim H, Didelot A, Charpentier MC, Bain S, Marmey B, Bonjour P, Biton J, Cremer I, Dieu-Nosjean MC, Sautès-Fridman C, Régnard JF, Laurent-Puig P, Alifano M and Damotte D. The new histologic classification of lung primary adenocarcinoma subtypes is a reliable prognostic marker and identifies tumors with different mutation status: the experience of a French cohort. Chest 2014; 146: 633-643.
[18] Yoshida Y, Nitadori JI, Shinozaki-Ushiku A, Sato J, Miyaji T, Yamaguchi T, Fukayama M and Nakajima J. Micropapillary histological subtype in lung adenocarcinoma of 2 cm or less: impact on recurrence and clinical predictors. Gen Thorac Cardiovasc Surg 2017; 65: 273-279.
[19] Tsubokawa N, Mimae T, Sasada S, Yoshiya T, Mimura T, Murakami S, Ito H, Miyata Y, Nakayama H and Okada M. Negative prognostic influence of micropapillary pattern in stage IA lung adenocarcinoma. Eur J Cardiothorac Surg 2016; 49: 293-299.
[20] Chen ZQ, Huang LS and Zhu B. Assessment of seven clinical tumor markers in diagnosis of non-small-cell lung cancer. Dis Markers 2018; 2018: 9845123.
[21] Ren X, Zhang Y, Lyu Y, Jin B, Guo H, Wu J, Li X and Liu X. Lactate dehydrogenase and serum tumor markers for predicting metastatic status in geriatric patients with lung adenocarcinoma. Cancer Biomark 2019; 26: 139-150.
[22] Pujol JL, Boher JM, Grenier J and Quantin X. Cyfra 21-1, neuron specific enolase and prognosis of non-small cell lung cancer: prospective study in 621 patients. Lung Cancer 2001; 31: 221-231.
[23] Fu L, Wang R, Yin L, Shang X, Zhang R and Zhang P. CYFRA21-1 tests in the diagnosis of non-small cell lung cancer: a meta-analysis. Int J Biol Markers 2019; 34: 251-261.
[24] Tiseo M, Ardizzoni A, Cafferata MA, Loprevite M, Chiaramondia M, Filiberti R, Marroni P, Grossi F and Paganuzzi M. Predictive and prognostic significance of neuron-specific enolase (NSE) in non-small cell lung cancer. Anticancer Res 2008; 28: 507-13.
[25] Zong Q, Zhu F, Wu S, Peng L, Mou Y, Miao K, Wang Q, Zhao J, Xu Y and Zhou M. Advanced pneumonic type of lung adenocarcinoma: survival predictors and treatment efficacy of the tumor. Tumori 2021; 107: 216-225.
[26] Hegedűs F, Zombori-Tóth N, Kiss S, Lantos T and Zombori T. Prognostic impact of the IASLC grading system of lung adenocarcinoma: a systematic review and m eta-analysis. Histopathology 2024; 85: 51-61.
[27] Bai H, Meng S, Xiong C, Liu Z, Shi W, Ren Q, Xia W, Zhao X, Jian J, Song Y, Ni C, Gao X and Li Z. Preoperative CECT-based radiomic signature for predicting the response of Transarterial Chemoembolization (TACE) therapy in hepatocellular carcinoma. Cardiovasc Intervent Radiol 2022; 45: 1524-1533.
[28] Wang HC, Wang ZM, Hu WD, Liang XQ and Cui LL. Correlation of FDG PET/CT, tumor markers and Ki-67 index with EGFR mutation or positive ALK expression in patients with non-small cell lung cancer. Q J Nucl Med Mol Imaging 2024; 68: 169-175.
[29] Tu B, Wu J, Zhang W, Tang H, Dai T and Xie B. A novel cancer-associated membrane signature predicts prognosis and therapeutic response for lung adenocarcinoma. Sci Rep 2025; 15: 25482.
[30] Li S, Zeng Z, Hong Z, Li J and Xie C. The heterogeneous expression patterns of serum tumor markers in non-small cell lung cancer patients are predictive factors for progression-free survival. Discov Oncol 2025; 16: 1121.